

Bacterial community radial-spatial distribution in biofilms along pipe wall in chlorinated drinking water distribution system of East China

Jingqing Liu¹ · Hongxing Ren² · Xianbei Ye² · Wei Wang² · Yan Liu² · Liping Lou² · Dongqing Cheng³ · Xiaofang He⁴ · Xiaoyan Zhou⁴ · Shangde Qiu⁴ · Liusong Fu² · Baolan Hu²

Received: 4 July 2016 / Revised: 11 September 2016 / Accepted: 22 September 2016 / Published online: 19 October 2016
© Springer-Verlag Berlin Heidelberg 2016

Abstract Biofilms in the pipe wall may lead to water quality deterioration and biological instability in drinking water distribution systems (DWDSs). In this study, bacterial community radial-spatial distribution in biofilms along the pipe wall in a chlorinated DWDS of East China was investigated. Three pipes of large diameter (300, 600, and 600 mm) were sampled in this DWDS, including a ductile cast iron pipe (DCIP) with pipe age of 11 years and two gray cast iron pipes (GCIP) with pipe ages of 17 and 19 years, and biofilms in the upper, middle, and lower parts of each pipe wall were collected. Real-time quantitative polymerase chain reaction (qPCR) and culture-based method were used to quantify bacteria. 454 pyrosequencing was used for bacterial community analysis. The results showed that the biofilm density and total solid (TS) and volatile solid (VS) contents increased gradually from the top to the bottom along the pipe wall. Microorganisms were concentrated in the upper and lower parts of the pipe wall, together accounting for more than 80 % of the total biomass in the biofilms. The bacterial communities in biofilms were significantly different in different areas of the pipe wall and had no

strong interaction. Compared with the upper and lower parts of the pipe wall, the bacterial community in the middle of the pipe wall was distributed evenly and had the highest diversity. The 16S rRNA genes of various possible pathogens, including *Escherichia coli*, *Staphylococcus epidermidis*, *Pseudomonas aeruginosa*, and *Salmonella enterica*, were detected in the biofilms, and the abundances of these possible pathogens were highest in the middle of the pipe wall among three areas. The detachment of the biofilms is the main reason for the deterioration of the water quality in DWDSs. The results of this study suggest that the biofilms in the middle of the pipe wall have highly potential risk for drinking water safety, which provides new ideas for the study of the microbial ecology in DWDS.

Keywords Biofilms · Drinking water distribution system · Bacterial community · Radial-spatial distribution · Possible pathogens

Electronic supplementary material The online version of this article (doi:10.1007/s00253-016-7887-8) contains supplementary material, which is available to authorized users.

✉ Baolan Hu
blhu@zju.edu.cn

¹ College of Civil Engineering and Architecture, Zhejiang University, Hangzhou 310058, China

² Department of Environmental Engineering, Zhejiang University, Hangzhou 310058, China

³ Zhejiang Chinese Medical University, Hangzhou 310053, China

⁴ Shaoxing Water Environmental Science Institute Co. Ltd, Shaoxing 312000, China

Introduction

The safety of drinking water is closely related to human health (Tao and Xin 2014). Drinking water distribution systems (DWDSs) function to supply treated water safe for human consumption and comply with increasingly stringent quality regulations (Brookes et al. 2014). However, water quality deterioration was often observed in these systems, which was mainly associated with microbial instability (Liu et al. 2002; Nescerecka et al. 2014; El-Chakhtoura et al. 2015). Even if there is a certain content of residual chlorine in the bulk water, heterotrophic bacteria could grow depending on some organic matter, resulting in drinking water biological instability in the DWDS (Liu et al. 2015c).

Biofilms are found to be the primary source of microorganisms in DWDSs. Biofilms predominate because attached cells have certain advantages over suspended cells, such as the ability to metabolize recalcitrant organic compounds and increased resistance to chlorine and other biocides (Berry et al. 2006). If the flow shear stress at the pipe wall exceeds the normal daily values, the biofilms accumulated at the pipe wall and conditioned to the normal forces would be mobilized into the bulk water (Husband and Boxall 2011). The mobilization of biofilms from the pipe wall not only results in esthetically unacceptable discolored drinking water (Vreeburg and Boxall 2007) but also releases microorganisms into the network (Douterelo et al. 2014). Considering that biofilms have been associated with various problems in DWDS such as the water quality deterioration (Nescerecka et al. 2014), the hosting of possible pathogens (Ercumen et al. 2014), and the corrosion of pipes (Masters et al. 2014), further research is needed to fully understand these ecosystems.

It is reported that the microbial community in biofilms was influenced by many factors, such as pipe material (Ren et al. 2015), hydraulic condition (Douterelo et al. 2013), nutrient availability (Park and Hu 2010), type and concentration of disinfectant (Mi et al. 2015), and temperature (Pinto et al. 2014). It is found that the densities of bacteria on iron pipes were higher than that on plastic-based materials (PE and PVC) in a simulated DWDS (Niquette et al. 2000). Ren et al. found that the biofilm tended to accumulate in iron pipes, such as ductile cast iron pipe (DCIP) and gray cast iron pipe (GCIP), rather than stainless steel clad pipe (SSCP) and polyvinyl chloride (PVC) in an actual DWDS (Ren et al. 2015). It was reported that the composition and diversity of the bacterial community in 28-day-old biofilms were affected by different hydraulic regimes with a tendency of higher species richness and diversity detected at highly varied flows (Douterelo et al. 2013). *Gammaproteobacteria* were the predominant group (>65 %) within the biofilms formed under low varied flow condition, while *Betaproteobacteria* were abundant (>56 %) under steady state condition (Douterelo et al. 2013). The content of organic carbon in water played an important role in microorganism growth in most DWDSs (Ohkouchi et al. 2013). The composition of the bacterial community in biofilms was influenced by the type of disinfectant (Gagnon et al. 2005), and the ammonia-oxidizing microorganisms had high abundance in chloraminated DWDSs (Wang et al. 2014). Pinto et al. found that the characteristics of the microbial community had seasonal variation in DWDSs and the observed temporal trends were due largely to the shift in bacterial communities from cluster 2 (summer cluster) to cluster 1 (winter cluster) (Pinto et al. 2014).

In recent years, the spatial distribution of the microbial community in the DWDSs and the interaction of microorganisms in different phases attracted more attention, but the reported research was yet limited (Proctor and Hammes 2015).

The fluid-particle system in terms of mesoscopic dynamics can be described through a mixed lattice Boltzmann (LB) and cellular automata (CA) model (Chopard et al. 2000). As shown in Fig. 1, the particles including colloids and suspended solids in DWDSs are under a combined effect of flow rate and gravity. Colloids and suspended microorganisms at the nanoscale are subject to the random wandering of Brownian motion, while the particles with high density and big size keep moving down until they settle on the lower part of the pipe wall under the effect of gravity. If the local fluid flow is fast enough, the particles located in the pipe wall will be detached and moved further away. Otherwise, if the flow is slow, the resulting motion will be to land again. Liu et al. investigated the bacteria from four critical phases of an unchlorinated DWDS, including bulk water, pipe wall biofilms, suspended solids, and loose deposits. It was found that the bacteria associated with loose deposits and pipe wall biofilms that accumulated in the DWDS accounted for over 98 % of the total bacteria, and the bacteria in bulk water dominated by *Polaromonas* spp. were clearly different from that in the other three phases dominated by *Sphingomonas* spp. (Liu et al. 2014). To date, the study about the radial-spatial distribution of the microbial community in the pipe wall was rarely reported, and the microbial community in the middle area of the pipe wall was never concerned.

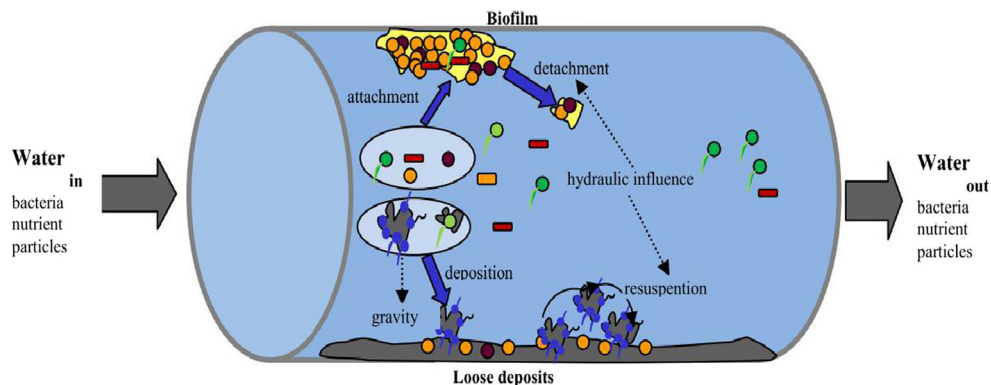
In this study, three pipes with pipe age more than 10 years, including one section of DCIP with diameter of 300 mm and two sections of GCIP with diameter of 600 mm, were obtained from a city DWDS in East China. Biofilms located at the upper, middle, and lower parts of the pipe wall from each pipe were sampled and investigated. This study aimed to investigate (1) the radial-spatial distribution of microbial biomass in biofilms along the pipe wall, (2) the radial-spatial distribution of bacterial community composition and structure in biofilms along the pipe wall; (3) and the relevance of the bacterial community in biofilms located in the upper, middle, and lower parts of the pipe wall.

Materials and methods

The drinking water distribution system

This study was performed in a city DWDS supplied by reservoir water in a town, in East China. The drinking water treatment plant employs the process of flocculation followed by sand filtration and chlorination before discharging to the DWDS, and the water treatment plant, with a drinking water yield of 500,000 m³/day, supplies 2,000,000 people. The treated water quality meets the national drinking water standards (Ren et al. 2015). As shown in Table S1, three pipes (L1-DCIP, L2-GCIP, L3-GCIP) located at the main pipelines of the DWDS were sampled during September 2013 to

Fig. 1 Particle-related processes across various phases (planktonic, biofilms, and particle-associated) in a drinking water distribution system. Adapted from (Vreeburg and Boxall 2007; Proctor and Hammes 2015)



November 2013. The service time of these pipes was 11, 17, and 19 years, respectively. As shown in Table S2, the flow rates in these locations ranged from 0.05 to 0.30 m/s, and the content of residual chlorine in bulk water ranged from 0.25 to 0.39 mg/L.

Biofilm sampling and pretreatment

Before cutting the pipe, water supply of the location was cut off and water in pipes was drained off slowly at a flow rate of less than 0.03 m/s to prevent biofilm drop-off. Then, soil around the sampling pipes was excavated and the surface of the pipe was physically decontaminated with tap water. As shown in Fig. 2, the upper and lower parts of the pipe were marked, and the pipe wall was divided into three equal areas with sterile cotton yarn by measuring the pipe diameter. The biofilms in each area was collected respectively by swabbing the inner pipe wall with a sterile brush while continuously washing the pipe wall with sterile water, and were then

transported to the laboratory in an ice box within 4 h. As described before (Ren et al. 2015), the biofilms were pretreated by the processes of shaking, filtration, centrifugation, and resuspension and were finally split into two parts: one (biofilm mass measured) was stored at $-80\text{ }^{\circ}\text{C}$ for DNA extraction, and the other was resuspended with remained supernatant and stored at $4\text{ }^{\circ}\text{C}$ for measurements of physico-chemical parameters and incubation experiment.

Physicochemical properties of biofilm analysis

The contents of total solids (TS), volatile solids (VS), iron, and manganese of the biofilms were determined (APHA 2012).

Bacteria quantification

Resuspended biofilm slurry (volume of 20 mL) was shaken in a sterile glass bottle (volume of 50 mL) with sterile glass beads (4–5 mm) for 15 min on a shaker before culturing. An equal

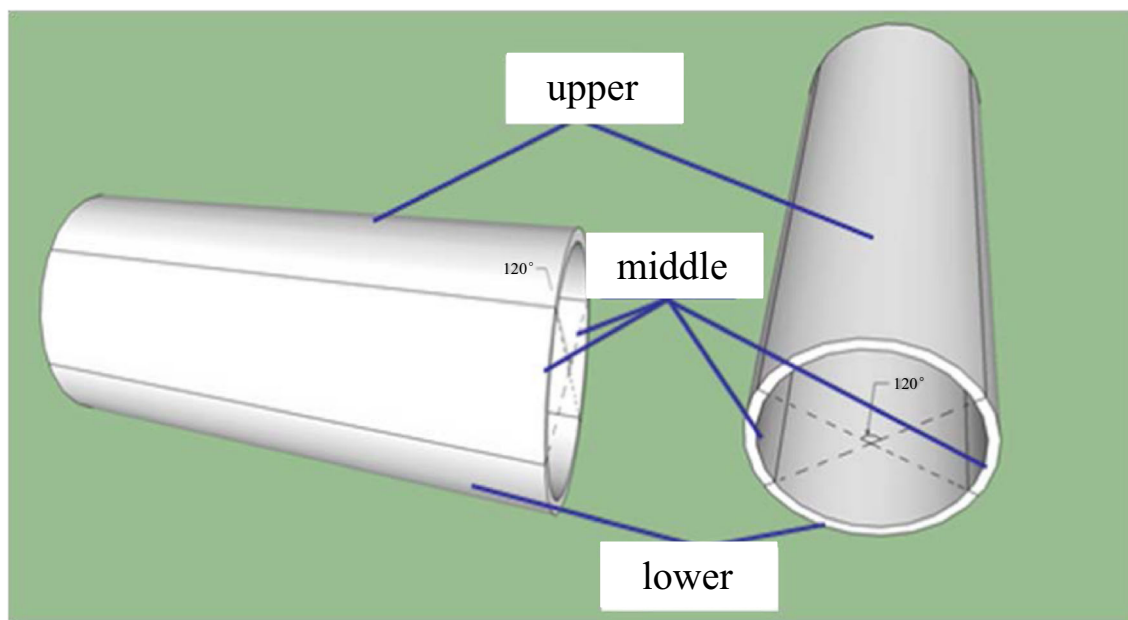


Fig. 2 Schematic diagram of biofilm sampling

volume of sterile water was used for control. The number of heterotrophic plate count (HPC) bacteria was determined by using the spread plate method with R2A agar and a 7-day incubation period at 25 °C (Reasoner and Geldreich 1985; Thayanukul et al. 2013). Total DNA was extracted from the biofilm (0.25 g) using a PowerSoil DNA Kit (Mo Bio Laboratories, Carlsbad, CA, USA), as described by the manufacturer. Quantitative PCR (qPCR) was used to quantify total bacteria in biofilm samples. qPCR was performed using an iCycler iQ5 thermocycler (Bio-Rad, CA). Forward primer 338F 5'-ACTCCTACGGGAG GCAGCAG-3' (Lane et al. 1991) and reverse primer 518R 5'-ATTACCGCGGCT GCTGG-3' (Muyzer et al. 1993) were chosen. The reaction systems and conditions were previously reported (Hu et al. 2014).

Pathogen database construction

Pathogenic bacteria species were selected according to HPB virulence factor database (<http://www.mgc.ac.cn/VFs/>) and used according to pathogen SEED database (Guo and Zhang 2012). Then, the 16S ribosomal RNA (rRNA) genes of these species were downloaded from NCBI's nonredundant and environmental databases (<http://www.ncbi.nlm.nih.gov>). As a quality control step, sequences that were shorter than 1000 bp were removed. The final pathogen database contained 112 sequences corresponding to 112 species of pathogenic bacteria.

454 pyrosequencing

Total DNA was used for bacterial 16S rRNA gene pyrosequencing to analyze bacterial community composition. The primer pairs 357F (5'-CCTACGGG AGGCAGCAG-3') and 926R (5'-CCGTCAATTCMTTTRAGT-3') were used to amplify the V3–V5 region of the bacterial 16S rRNA genes. A barcode was permuted for each sample to allow for the identification of individual samples in a mixture within a single pyrosequencing run. The detailed protocol was reported by Ren et al. (2015). All of the samples were quantified by TBS-380 and mixed at an equimolar ratio in a single tube to be run on a Roche FLX+ 454 pyrosequencing system (Roche Diagnostics Corporation, Branford, CT, USA).

Data analysis

Sequences generated from the pyrosequencing were subsequently processed using the Mothur software package (<http://www.mothur.org>). After denoising and chimera inspection, 15,000 high-quality sequence reads (quality score >25, exact matching to barcode and primer, 200–800 bp in length, and containing no chimeras) were

randomly selected from each sample. The high-quality sequences of each sample were compared with the pathogen database using BLAST with an E-value $<1 \times 10^{-7}$ at a 97 % sequence identity threshold to detect possible pathogens in biofilms. In addition, operational taxonomic units (OTUs) were generated using a 97 % sequence identity threshold (Schloss and Handelsman 2005). Representative OTUs were selected based on the most abundant sequence, and taxonomic assignment was conducted using the Ribosomal Database Project (RDP) classifier with data sets from the RDP pyrosequencing pipeline (Cole et al. 2009). Finally, the Chao and Shannon diversity indices and coverage were calculated. The ecological distribution of the biofilm communities and their associations with environmental factors were determined using principal components analysis (PCA) and canonical correspondence analysis (CCA), respectively, using CANOCO software based on normalized values of the abundance of each OTU in biofilm samples (Shen et al. 2013). A Pearson correlation analysis (significance level $p < 0.05$) was used to test the correlations between physicochemical and biotic factors (Liu et al. 2015b). One-way ANOVA was used to determine whether the biofilm samples had significant difference (Shen et al. 2013).

Data accession number

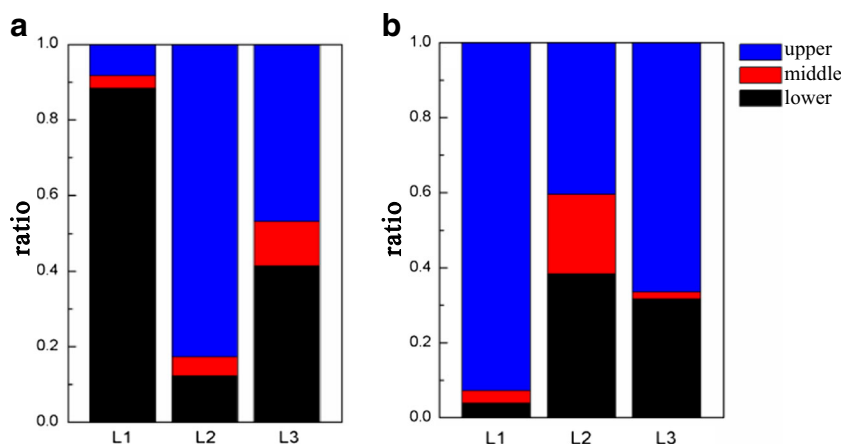
Raw sequences are available from the NCBI Sequence Read Archive (SRA accession number: PRJNA328456).

Results

Physicochemical properties of biofilm

As shown in Table 1, the densities of biofilms accumulated on pipe walls ranged from 39.56 to 55.06 mg/cm² and increased gradually from the top to the bottom along the pipe wall. The densities of biofilms in the lower part of the pipe wall were 1.46, 1.57, and 1.13 times more than that in the upper part of the pipe wall in L1-DCIP, L2-GCIP, and L3-GCIP, respectively. The concentrations of TS and VS ranged from 12.71 to 38.40 mg/cm² and from 0.72 to 2.41 mg/cm², respectively. The concentrations of TS and VS in L1-DCIP and L2-GCIP increased from the top to the bottom along the pipe wall, while in L3-GCIP, the concentrations of TS and VS were the highest in the upper part. The contents of Fe and Mn in biofilms ranged from 1.06 to 3.77 mg/cm² and from 0.02 to 2.71 mg/cm², respectively, and the contents of Fe and Mn in biofilms increased from the top to the bottom in pipes, which were consistent with the biofilm mass. Moreover, correlation analysis, according to Pearson test, showed that there

Fig. 3 Comparison of bacterial abundance (comparison of biomass as inferred from q-PCR (a) and HPC (b) in biofilms). The results are shown in percentage of different biofilms to the overall amount of bacteria in the pipe wall



was a significantly positive correlation between VS, Fe, and Mn and between biofilm density and Mn with $p < 0.01$ (Table S3, sample numbers = 9).

Bacteria quantity in biofilms

In this study, the bacterial 16S rRNA gene copies in biofilms ranged from 10^6 to 10^8 gene copies per square centimeter, and HPC ranged from 10^5 to 10^7 CFU/cm². As quantified by q-PCR and HPC, the lowest biomass was found in the middle of the pipe wall, with q-PCR ranging from 5.7×10^6 to 8.5×10^7 copies/cm² and HPC ranging from 1.0 to 6.0×10^5 CFU/cm² in three pipes. In the upper and lower parts of the pipe wall from three pipes, the q-PCR and HPC had the value of 6.5×10^6 – 3.4×10^8 copies/cm² and 1.8×10^5 – 2.7×10^7 CFU/cm², respectively (Table S4). A difference of the value of qPCR and HPC in different areas of the pipe wall was found by using one-way ANOVA test with $p < 0.05$ (Table S5). The comparison of bacterial abundance in different areas of the pipe wall was performed on the basis of q-PCR and HPC measurements, and the results were represented as percentage in Fig. 3. As shown, the biomass in biofilms was concentrated in the upper and lower parts of the pipe wall, together accounting for 80–98 % of the overall q-PCR and HPC in the pipe wall.

Table 1 Physicochemical properties of biofilms

Sample-ID		TS (mg/cm ²)	VS (mg/cm ²)	Density of biofilms (mg/cm ²)	Fe (mg/cm ²)	Mn (mg/cm ²)
L1-DCIP	Upper	16.65	1.67	45.16	1.89	0.60
	Middle	16.78	1.96	46.31	2.78	0.97
	Lower	25.56	2.41	66.06	3.77	2.71
L2-GCIP	Upper	12.71	0.78	39.56	2.01	0.34
	Middle	22.42	1.07	54.98	2.24	0.84
	Lower	21.20	1.63	62.27	2.96	1.82
L3-GCIP	Upper	38.40	1.25	46.62	1.13	0.03
	Middle	22.29	0.72	45.01	1.06	0.02
	Lower	25.47	0.81	52.51	1.57	0.06

Bacterial community diversity of biofilms

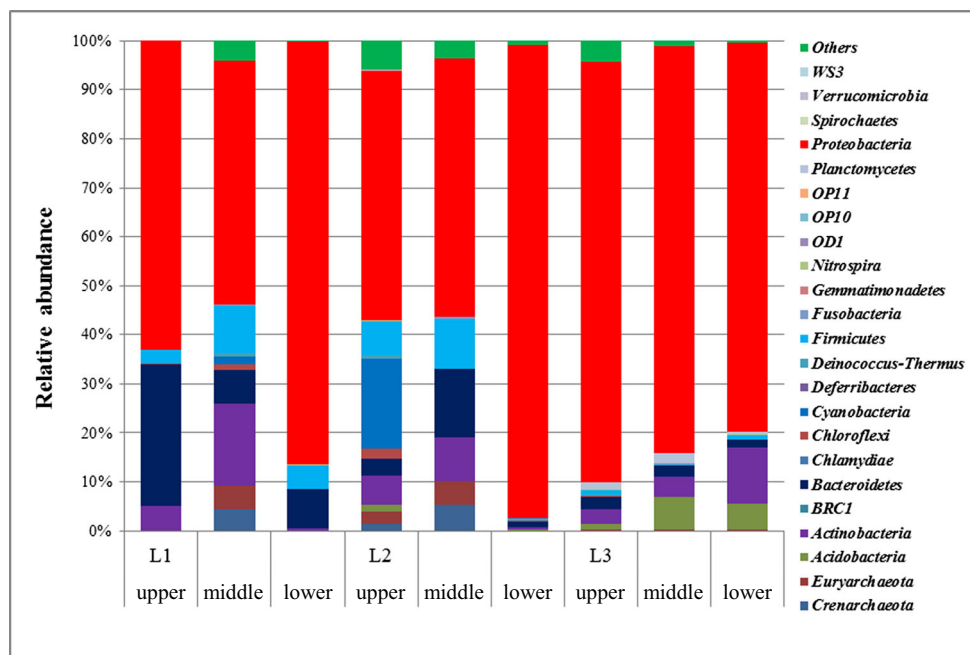
A total of 184,449 high-quality sequences were obtained from nine biofilm samples, and 15,000 high-quality sequences were randomly selected from each sample and used for analysis. Sample coverage reached 98 %, suggesting that medium-depth pyrosequencing captured the majority of unique bacterial OTUs.

The species richness and evenness of communities were evaluated by Chao and Shannon indices. As shown in Table S6, the biofilms in the middle of the pipe wall had a Chao index less than that in the upper and lower parts of the pipe wall, which showed that richness of bacterial communities in the middle of the pipe wall was the lowest. However, the biofilms in the middle of the pipe wall had the highest Shannon index among three areas, suggesting that the bacterial community in the middle of the pipe wall was distributed most evenly.

The bacterial composition and structure in biofilms

As shown in Fig. 4, sequences in biofilms in this study were assigned to 21 phyla, including *Proteobacteria*, *Bacteroidetes*, *Actinobacteria*, *Firmicutes*, and *Cyanobacteria*, and the phylum *Proteobacteria* were the

Fig. 4 Relative abundance of different phyla in biofilms



dominant bacterial communities (50–97 %) among all samples. In addition, sequences assigned to *Euryarchaeota* and *Crenarchaeota* were also detected, accounting for about 1.3 % among the total sequences. In L1-DCIP, the relative abundances of *Proteobacteria* were 63, 50, and 87 % in the upper, middle, and lower parts of the pipe wall, respectively, and in L2-GCIP, the numbers were 51, 53, and 97 %, which showed that there was a significant difference in the bacterial community at the phylum classification among different areas of the pipe wall in both pipes. Inconsistently, L3-DCIP biofilms had the similar abundances of *Proteobacteria* in different areas of the pipe wall, with 87, 84, and 80 % in the upper, middle, and lower parts, respectively.

A heat map about the distribution of 30 genera of the highest abundance in biofilms showed a significant difference among the bacterial community from different areas of the pipe wall (Fig. 5). In biofilms from the upper and lower parts of the pipe wall, the bacterial community was dominated by a few species. In L1-DCIP, the bacterial community was dominated by *Pseudomonas*, *Flavobacterium*, and *Cellvibrio* in the upper and lower parts, accounting for 10–20 % of the total sequences. In L2-GCIP, the bacterial community was dominated by *Methylobacterium* (21 %) or *Comamonadaceae* (89 %) in the upper and lower parts. In the upper part of L3-GCIP, an unclassified OTU assigned to *Rhodocyclaceae* accounted for 45 % of total sequences. Compared with the upper and lower parts of the pipe wall, the bacterial community in the middle was distributed evenly. More than 20 genera accounted for more than 1 % of the total sequences, including *Pseudomonas*, *Sphingomonas*, and *Hyphomicrobium*.

A CCA was performed to test the relationship between the environmental factors and bacterial community composition

(Fig. 6) with p value, shown in Table S7 in the Supplementary Material. The CCA results indicated that the biofilms from one pipe are more likely to have the same bacterial community structure. The total iron content of biofilms and TS was the most significant factor influencing the bacterial community distribution of biofilm ($p < 0.05$, 498 Monte Carlo permutations, sample numbers = 9). In addition, the content of Mn was correlated with the bacterial community composition, although this effect did not reach a significant level.

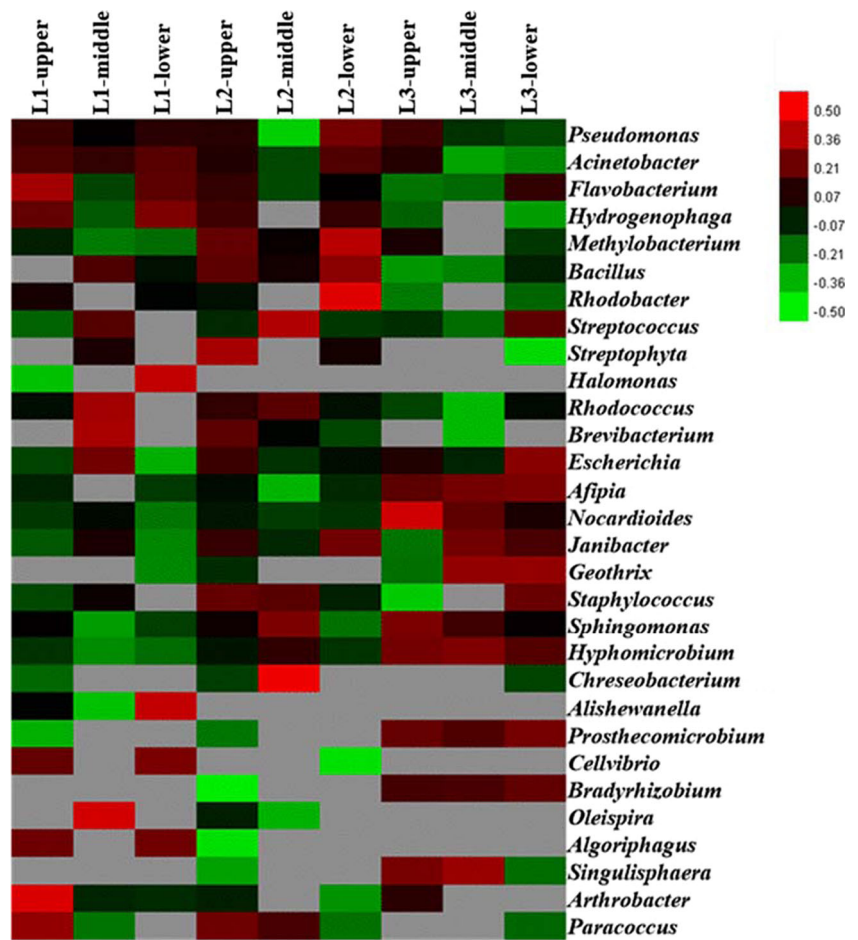
Core microbiome

OTU characteristics of the biofilm samples are shown in Fig. S1. In the three pipes, the biofilms harbored a larger number of unique OTUs, thus showing greater bacterial richness. The number of OTUs in DCIP was 493, less than that in GCIP of 1120 and 1485, and the number of OTUs in the upper part of the pipe wall was more than that in other areas. On the other hand, less than 16 % of the OTUs were found in different areas of the pipe wall in all pipes. This small fraction of common taxa, including *Pseudomonas*, *Sphingomonas*, *Flavobacterium*, *Escherichia coli*, *Hyphomicrobium*, *Janibacter*, and *Nocardioideis*, constituted the core microbiome for this DWDS.

Possible pathogens in biofilms

The high-quality sequences from pyrosequencing were compared against the pathogen database for possible pathogen determination, and the results are shown in Table 2. The sequences assigned to *E. coli*, *Staphylococcus epidermidis*, *Streptococcus pneumoniae*, *Brucella melitensis*,

Fig. 5 Heat map showing the percentages of the 30 most abundant species at the genus level in biofilms from different sites along the pipe wall. The data (percentages of each species) were adjusted by log transformation and median centralization and normalization, and the value presented in the color bar was positively correlated with the real value of the species abundance



Pseudomonas aeruginosa, *Mycobacterium ulcerans*, *Salmonella enterica*, *Staphylococcus aureus*, and *Acinetobacter calcoaceticus* were detected in biofilms. The detection rate of *E. coli* was 100 % among all samples, and the detection rates of *S. epidermidis*, *S. pneumoniae*, and *B. melitensis* also reached more than 44 %. *Escherichia coli* were also the most abundant with an average abundance of 1.39 % among all samples, and the highest abundance (7.60 %) was found in the middle of L1-DCIP. Comparing the distribution of possible pathogens in different areas, the results showed that the detection rate of possible pathogens in the upper and middle parts of the pipe wall was higher than that in the lower part, and the average abundance of possible pathogens was the highest in the middle of the pipe wall.

Discussion

Radial-spatial distribution of biofilm accumulation along the pipe wall

In this study, the densities of the biofilm from three iron pipes ranged from 40 to 50 mg/cm² and the contents of TS and VS

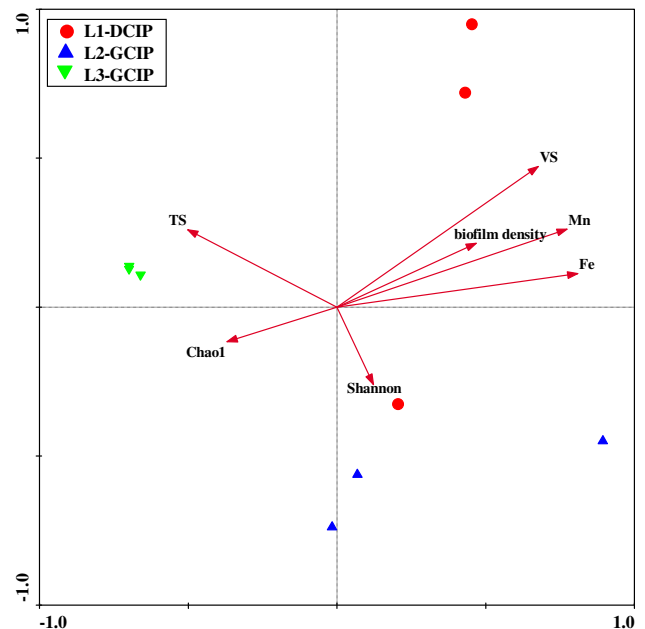


Fig. 6 CCA ordination plots for the first dimensions showing the relationship between the biofilm bacterial community structure and physicochemical properties and diversity index

Table 2 Possible pathogens in biofilms determined by sequences from pyrosequencing

Sample ID	L1-DCIP			L2-GCIP			L3-GCIP		
	Upper	Middle	Lower	Upper	Middle	Lower	Upper	Middle	Lower
<i>Escherichia coli</i>	+	7.6 %	+	+	+	+	++	++	+
<i>Staphylococcus epidermidis</i>	+	+	–	+	–	+	+	+	+
<i>Streptococcus pneumoniae</i>	+	+	–	–	–	+	+	++	+
<i>Brucella melitensis</i>	–	+	–	–	+	–	+	+	–
<i>Pseudomonas aeruginosa</i>	–	–	–	–	–	–	+	–	+
<i>Mycobacterium ulcerans</i>	–	–	–	+	–	–	+	–	–
<i>Salmonella enterica</i>	–	–	–	–	–	–	+	–	–
<i>Staphylococcus aureus</i>	–	–	–	–	–	–	+	+	–
<i>Acinetobacter calcoaceticus</i>	–	–	–	–	–	–	–	–	–

++ with relative abundance more than 1 %, + with relative abundance between 0 and 1 %, – no detection

in biofilms ranged from 12 to 39 mg/cm² and from 0.7 to 2.4 mg/cm², respectively, which were consistent with previous research results of this DWDS (Ren et al. 2015), but more than that reported in other DWDSs (Barbeau et al. 2005; Vreeburg et al. 2008; Liu et al. 2014), as a result of the influence of a variety of factors such as particle load (Liu et al. 2013a, b), hydraulic condition (Douterelo et al. 2013), and pipe material and pipe age (Zhu et al. 2014). Liu et al. found that the particle size in biofilms increased gradually from the top to the bottom of the pipe wall, as the particles with large size were strongly under the influence of gravity and deposited to the bottom (Liu et al. 2015a). As expected, the densities of biofilms and the content of TS and VS increased gradually from the top to the bottom of the pipe wall in this study. Various dissolved substances and particles do enter DWDS within the bulk flow, and these substances and particles can accumulate, forming biofilms attached to the internal surfaces of pipes (Vreeburg and Boxall 2007). In general cases, colloids and suspended microorganisms at the nanoscale are subject to random wandering of Brownian motion, while the particles with high density and size keep moving downward until they land on the lower part of the pipe wall under the effect of gravity (Young and Leeming 1997). Moreover, the contents of Fe and Mn in biofilms located in the lower part of the pipe wall were the highest among the pipe wall. The results of Pearson test showed that the contents of Fe and Mn were significantly correlated with the contents of VS, representing the biomass of biofilms. Microorganisms had important contribution for iron pipe corrosion (Farkas et al. 2013). It was reported that a serious corrosion was detected in the iron pipes with high quantity and strong activity of microorganisms (Yang et al. 2014). In addition, the densities of biofilms in the lower part

of the pipe wall were the highest and the particles might carry Fe and Mn, resulting in more contents of Fe and Mn in this area (Yang et al. 2014). In turn, the increased contents of Fe and Mn had an effect in bacterial abundance and composition in biofilms (Liu et al. 2015a).

Radial-spatial distribution of bacterial community

Biofilms is the main place for the growth of microorganisms in DWDSs (Liu et al. 2013b; Proctor and Hammes 2015). In addition to bacteria, archaea were also detected in biofilms by pyrosequencing, which was due to gene homology between bacteria and archaea and the specificity of the amplification primers used in this study (GM et al. 2005). The same primers were used to amplify the rRNA 16S gene in the previous study, and a small number of sequences assigned to archaea were detected (Ren et al. 2015). The total bacterial 16S rRNA gene abundance in biofilms from pipes ranged from 10⁶ to 10⁸ gene copies per square centimeter, and the number of culturable heterotrophic bacteria ranged from 10⁵ to 10⁷ CFU/cm². Both qPCR and HPC values are consistent with that previously reported (Liu et al. 2013b). There was a difference in the number of bacteria in the biofilms from different pipes, which was influenced by the sampling location, pipe age, and water quality (van der Kooij and van der Wielen 2014).

In the DWDSs, the microorganisms had continuous interaction among different phases (Proctor and Hammes 2015). Up to now, the study about the radial-spatial distribution of the bacterial community in biofilms was little reported. The sediment located in the pipe wall was divided into loose deposits (the surface layer of sediment) and biofilms (the deep layer of

sediments) by Liu et al., and the bacteria from four critical phases, including bulk water, pipe wall biofilm, suspended solids, and loose deposits, were quantified and identified by adenosine triphosphate analysis and pyrosequencing, respectively, in an unchlorinated DWDS (Liu et al. 2014). It was reported that bacteria associated with biofilms and loose deposits accounted for over 98 % of the total bacteria in the DWDS, which proved the importance of biofilms located in the pipe wall. In this study, the biofilms in the pipe wall were particularly divided into the upper, middle, and lower parts of the pipe wall according to the rule of particle sedimentation. The biofilms in the three pipes harbored a larger number of OTUs, showing greater bacterial richness. Surprisingly, the bacterial community in different areas of the pipe wall had low similarity and the core OTUs in biofilms only accounted for less than 16 % of the whole OTUs. That is to say, the different genera in biofilms were inhabited in different niches. Moreover, a significant difference ($p < 0.01$) of bacterial quantity and composition of the bacterial community in different areas of the pipe wall was found in this study, suggesting that different phases might be present in biofilms along the pipe wall, which were suitable for unique microorganism growth.

Despite that the relative amount of bacteria in biofilms differed in different pipes, which was related to the sampling location (Liu et al. 2014), the number of bacteria in the upper and lower parts of the pipe wall was significantly higher than that in the middle of the pipe wall, together accounting for more than 80 % of the biomass in the whole pipe wall. In biofilms located in the upper part of the pipe wall, the bacterial community was dominated by *Pseudomonas*, *Flavobacterium*, and *Acinetobacter*, which were often detected in DWDSs to form biofilms (Lin et al. 2013; Ren et al. 2015). In biofilms in the lower part of the pipe wall, the bacterial community was dominated by *Cellvibrio*, *Comamonadaceae*, or *Rhodocyclaceae*, which were commonly detected in the soil environment (GM et al. 2005), and these microorganisms might be carried by particles from the drinking water plant (El-Chakhtoura et al. 2015). Compared with the upper and lower parts of the pipe wall, the bacterial community in the middle was distributed evenly with the highest bacterial community diversity. More than 20 genera with relative abundance of more than 1 %, including *Pseudomonas*, *Sphingomonas*, and *Hyphomicrobium*, were detected in biofilms in the middle of the pipe wall.

For the same pipe section, the water quality, temperature, and pipe materials are all consistent. Therefore, gravity, water flow, and particle deposition are the main reasons for the bacterial community distribution along the pipe wall. As expected, the biofilms in the lower part of the pipe wall had more biomass, as particles carrying microorganisms accumulated in the area were the most abundant under the condition of gravity (Liu et al. 2014). Surprisingly, the biomass of biofilms in the upper part of the pipe wall was as much as that in the lower

part, while the biomass of biofilms in the middle part of the pipe wall was the least among different areas. It might be that the biofilms attached to the upper part of the pipe wall had to have enough biomass to have good adhesion property, preventing themselves from being washed off and from falling off into the water body (Gomes 2013). Compared with the upper and lower parts of the pipe wall, the biofilms in the middle had the least biomass but with the highest level of diversity, because the particles accumulating in this area were easily moved up and down under the condition of flow fluctuation and had frequent interaction with suspended particles in bulk water (Young and Leeming 1997).

Radial-spatial distribution of possible pathogens in biofilms

Unluckily, the sequences assigned to *E. coli*, *S. epidermidis*, *S. pneumoniae*, *B. melitensis*, *P. aeruginosa*, *M. ulcerans*, *S. enterica*, *S. aureus*, and *A. calcoaceticus* were detected in biofilms. As we know, biofilms are always present in DWDSs. During the process of drinking water from water plant to the top, biofilms in the pipe wall would fall off into bulk water due to certain reasons, including the natural biofilm growth succession and hydraulic fluctuation of water flow (Proctor and Hammes 2015). Seriously, possible pathogens in the biofilms would fall off and be exposed into water with biofilm detachment and then threaten human health (Buse et al. 2012).

Escherichia coli, commonly used to evaluate the microbial safety of drinking water, were detected in all samples with the highest abundance in this study (Table 2). Compared with the upper and lower parts of the pipe wall, the abundance of possible pathogens was the highest in the middle of the pipe wall. In this study, the percentage of *E. coli* was highest in the biofilm in the middle of L1-DCIP, accounting for 7.60 % of the total bacteria. Considering the frequent interaction between biofilms in the middle of the pipe wall and the bulk body, the biofilms in this area played an important role in drinking water safety, which needs to be paid more attention.

In this study, the radial-spatial distribution of the bacterial community in biofilms along the pipe wall of large-diameter pipes in the DWDS was investigated and three different microbial phases in biofilms along the pipe wall was found. The biofilm density and the TS and VS contents increased gradually from the top to the bottom along the pipe wall. The biomass was concentrated in the upper and lower parts of the pipe wall, both areas accounting for more than 80 % of the total bacteria in the pipe wall. Compared with that in the upper and lower parts of the pipe wall, the structure of the bacterial community in the middle was distributed evenly, and the bacterial community diversity level was the highest. A variety of possible pathogens were detected in biofilms. Compared with that in the upper and lower parts of the pipe wall, the possible pathogen abundance was the highest in the middle. The results

of this study suggest that the biofilms in the middle of the pipe wall had a highly potential risk for drinking water safety, which provides new ideas for the study of the microbial ecology in DWDS. However, in this study, only one pipe of each sampling site was collected, and a more comprehensive study on the radial-spatial distribution of the bacterial community in biofilms in DWDSs should be performed.

Acknowledgments This work was supported by the Natural Science Foundation of China (No. 51378455) and the Key Special Program on the S&T of China for the Pollution Control and Treatment of Water Bodies (No. 2012ZX07403-003). This work was also supported by the biological information technology service platform at the Faculty of Agriculture, Life, and Environment, Zhejiang University.

Compliance with ethical standards

Ethical statement This article does not contain any studies with human participants or animals performed by any of the authors. Informed consent was obtained from all individual participants included in the study.

Conflict of interest The authors declare that they have no conflict of interest.

References

- APHA (2012) Standard methods for the examination of water and wastewater. American Public Health Association, Washington
- Barbeau B, Gauthier V, Julienne K, Carriere A (2005) Dead-end flushing of a distribution system: short and long-term effects on water quality. *J Water Supply Res T* 54(6):371–383
- Berry D, Xi C, Raskin L (2006) Microbial ecology of drinking water distribution systems. *Curr Opin Biotechnol* 17(3):297–302
- Brookes JD, Carey CC, Hamilton DP, Ho L, van der Linden L (2014) Emerging challenges for the drinking water industry. *Environ Sci Technol* 48(4):2099–2101
- Buse HY, Schoen ME, Ashbolt NJ (2012) Legionellae in engineered systems and use of quantitative microbial risk assessment to predict exposure. *Water Res* 46(4):921–933
- Chopard B, Alexandre M, Dupuis A (2000) A lattice gas model for erosion and particles transport in a fluid. *Comput Phys Commun* 129:167–176
- Cole JR, Wang Q, Cardenas E, Fish J, Chai B, Farris RJ, Kulam-Syed-Mohideen AS, McGarrell DM, Marsh T, Garrity GM, Tiedje JM (2009) The Ribosomal Database Project: improved alignments and new tools for rRNA analysis. *Nucleic Acids Res* 37:D141–D145
- Douterelo I, Sharpe RL, Boxall JB (2013) Influence of hydraulic regimes on bacterial community structure and composition in an experimental drinking water distribution system. *Water Res* 47(2):503–516
- Douterelo I, Husband S, Boxall JB (2014) The bacteriological composition of biomass recovered by flushing an operational drinking water distribution system. *Water Res* 54:100–114
- El-Chakhtoura J, Prest E, Saikaly P, van Loosdrecht M, Hammes F (2015) Dynamics of bacterial communities before and after distribution in a full-scale drinking water network. *Water Res* 74C:180–190
- Ercumen A, Gruber JS, Colford JM (2014) Water distribution system deficiencies and gastrointestinal illness: a systematic review and meta-analysis. *Environ Health Persp* 122(7):651–660
- Farkas A, Dragan-Bularda M, Muntean V, Ciataras D, Tigan S (2013) Microbial activity in drinking water-associated biofilms. *Cent Eur J Biol* 8(2):201–214
- Gagnon GA, Rand JL, O’Leary KC, Rygel AC, Chauret C, Andrews RC (2005) Disinfectant efficacy of chlorite and chlorine dioxide in drinking water biofilms. *Water Res* 39(9):1809–1817
- GM G, DJ B, NR K, JT S (2005) *Bergey’s manual of systematic bacteriology*. Springer Science & Business Media, Inc., New York
- Gomes IB (2013) Understanding the behavior of a drinking water biofilm model to chemical and mechanical stresses
- Guo F, Zhang T (2012) Profiling bulking and foaming bacteria in activated sludge by high throughput sequencing. *Water Res* 46(8):2772–2782
- Hu B, Shen L, Lian X, Zhu Q, Liu S, Huang Q, He Z, Geng S, Cheng D, Lou L, Xu X, Zheng P, He Y (2014) Evidence for nitrite-dependent anaerobic methane oxidation as a previously overlooked microbial methane sink in wetlands. *P Natl Acad Sci USA* 111(12):4495–4500
- Husband PS, Boxall JB (2011) Asset deterioration and discoloration in water distribution systems. *Water Res* 45(1):113–124
- Lane DJ, Weisburg WG, Barns SM (1991) 16S ribosomal DNA amplification for phylogenetic study. *J Bacteriol* 173(2):697–703
- Lin W, Yu Z, Xi C, Liu R, Zhang H (2013) Molecular characterization of natural biofilms from household taps with different materials: PVC, stainless steel, and cast iron in drinking water distribution system. *Appl Microbiol Biotechnol* 97(18):8393–8401
- Liu W, Wu H, Wang Z, Ong SL, Hu JY (2002) Investigation of assimilable organic carbon (AOC) and bacterial regrowth in drinking water distribution system. *Water Res* 36:891–898
- Liu G, Lut MC, Verberk JQJC, Van Dijk JC (2013a) A comparison of additional treatment processes to limit particle accumulation and microbial growth during drinking water distribution. *Water Res* 47(8):2719–2728
- Liu G, Verberk JQJC, Van Dijk JC (2013b) Bacteriology of drinking water distribution systems: an integral and multidimensional review. *Appl Microbiol Biotechnol* 97(21):9265–9276
- Liu G, Bakker GL, Li S, Vreeburg JH, Verberk JQ, Medema GJ, Liu WT, Van Dijk JC (2014) Pyrosequencing reveals bacterial communities in unchlorinated drinking water distribution system: an integral study of bulk water, suspended solids, loose deposits, and pipe wall biofilm. *Environ Sci Technol* 48(10):5467–5476
- Liu J, Chen H, Huang Q, Lou L, Hu B, Endalkachew SD, Mallikarjuna N, Shan Y, Zhou X (2015a) Characteristics of pipe-scale in the pipes of an urban drinking water distribution system in eastern China. *Water Sci Tech Water Supply*
- Liu S, Ren H, Shen L, Lou L, Tian G, Zheng P, Hu B (2015b) pH levels drive bacterial community structure in sediments of the Qiantang River as determined by 454 pyrosequencing. *Front Microbiol* 6:285
- Liu X, Wang J, Liu T, Kong W, He X, Jin Y, Zhang B (2015c) Effects of assimilable organic carbon and free chlorine on bacterial growth in drinking water. *PLoS One* 10(6)
- Masters S, Wang H, Pruden A, Edwards MA (2014) Redox gradients in distribution systems influence water quality, corrosion, and microbial ecology. *Water Res* 68C:140–149
- Mi Z, Dai Y, Xie S, Chen C, Zhang X (2015) Impact of disinfection on drinking water biofilm bacterial community. *J Environ Sci (China)* 37:200–205
- Muyzer G, de Waal EC, Uitterlinden AG (1993) Profiling of complex microbial populations by denaturing gradient gel electrophoresis analysis of polymerase chain reaction-amplified genes coding for 16S rRNA. *Appl Environ Microbiol* 59(3):695–700
- Nescerecka A, Rubulis J, Vital M, Juhna T, Hammes F (2014) Biological instability in a chlorinated drinking water distribution network. *PLoS One* 9(5):1–11

- Niquette P, Servais P, Savoie R (2000) Impacts of pipe materials on densities of fixed bacterial biomass in a drinking water distribution system. *Water Res* 34(6):1952–1956
- Ohkouchi Y, Ly BT, Ishikawa S, Kawano Y, Itoh S (2013) Determination of an acceptable assimilable organic carbon (AOC) level for biological stability in water distribution systems with minimized chlorine residual. *Environ Monit and Assess* 185(2):1427–1436
- Park SK, Hu JY (2010) Interaction between phosphorus and biodegradable organic carbon on drinking water biofilm subject to chlorination. *J Appl Microbiol* 108(6):2077–2087
- Pinto AJ, Schroeder J, Lunn M, Sloan W, Raskin L (2014) Spatial-temporal survey and occupancy-abundance modeling to predict bacterial community dynamics in the drinking water microbiome. *MBio* 5(3):e011135–e01114
- Proctor CR, Hammes F (2015) Drinking water microbiology—from measurement to management. *Curr Opin Biotechnol* 33:87–94
- Reasoner DJ, Geldreich EE (1985) A new medium for the enumeration and subculture of bacteria from potable water. *Appl Environ Microbiol* 49(1):1–7
- Ren H, Wang W, Liu Y, Liu S, Lou L, Cheng D, He X, Zhou X, Qiu S, Fu L, Liu J, Hu B (2015) Pyrosequencing analysis of bacterial communities in biofilms from different pipe materials in a city drinking water distribution system of East China. *Appl Microbiol Biotechnol* 99(24):10713–10724
- Schloss PD, Handelsman J (2005) Introducing DOTUR, a computer program for defining operational taxonomic units and estimating species richness. *Appl Environ Microbiol* 71(3):1501–1506
- Shen L, Liu S, Zhu Q, Li X, Cai C, Cheng D, Lou L, Xu X, Zheng P, Hu B (2013) Distribution and diversity of nitrite-dependent anaerobic methane-oxidising bacteria in the sediments of the Qiantang River. *Microb Ecol*
- Tao T, Xin K (2014) A sustainable plan for China's drinking water. *Nature* 511(7511):527–528
- Thayanukul P, Kurisu F, Kasuga I, Furumai H (2013) Evaluation of microbial regrowth potential by assimilable organic carbon in various reclaimed water and distribution systems. *Water Res* 47(1):225–232
- van der Kooij D, van der Wielen PWJJ (2014) Microbial growth in drinking-water supplies: problems, causes, control and research needs (IWA)
- Vreeburg JH, Boxall JB (2007) Discolouration in potable water distribution systems: a review. *Water Res* 41(3):519–529
- Vreeburg JHG, Schippers D, Verberk JQJC, van Dijk JC (2008) Impact of particles on sediment accumulation in a drinking water distribution system. *Water Res* 42(16):4233–4242
- Wang H, Masters S, Edwards MA, Falkinham JO, Pruden A (2014) Effect of disinfectant, water age, and pipe materials on bacterial and eukaryotic community structure in drinking water biofilm. *Environ Sci Technol* 48(3):1426–1435
- Yang F, Shi B, Bai Y, Sun H, Lytle DA, Wang D (2014) Effect of sulfate on the transformation of corrosion scale composition and bacterial community in cast iron water distribution pipes. *Water Res* 59:46–57
- Young J, Leeming A (1997) A theory of particle deposition in turbulent pipe flow. *J Fluid Mech* 340:129–159
- Zhu Z, Wu C, Zhong D, Yuan Y, Shan L, Zhang J (2014) Effects of pipe materials on chlorine-resistant biofilm formation under long-term high chlorine level. *Appl Biochem Biotechnol* 173(6):1564–1578